Analysis and Simulation of Energy Leakage for the Surface-Wave Waveguide Based on Tunable Impedance Cells

YongHong Zhou [1,2], Xing Chen [1], and ZhangJie Luo [3]

[1] College of Electronics and Information Engineering
Sichuan University, Chengdu, 610064, China
scnczyh@163.com, xingcsc@yahoo.com.cn

[2] College of Electronics and Information Engineering
China West Normal University, Nanchong, 637002, China
scnczyh@163.com

[3] Institute of Electronic Engineering
China Academy of Engineering Physics, Mianyang, 621900, China
zhangjie_luo_cn@126.com

Abstract ─ Controlling energy leakage is of great importance for users of surface-wave waveguides (SWGs) because it determines the propagating efficiency of surface waves. In this paper, a novel theoretical analysis of the energy leakage for these two types of SWGs is proposed, and the effects of some key parameters to the leakage such as the path width of the SWG and effective impedance of cell and incident angle are discussed more deeply. To verify the theoretical method, a model of the SWG consisting of 30 × 30 impedance-tunable cells driven by TM surface waves, whose impedance ranges from j370 Ω to j780 Ω according to our previous measurements, is simulated in HFSS. The simulation results are in good agreement with the theoretical ones, demonstrating that the leakage is inversely proportional to the width of the SWG and an increase of effective impedance of the guided path; furthermore, by using the impedance-tunable cells, the multi-functionality of the SWG is illustrated. The analyzing methods can be a guide for designing other SWGs without energy leakage, and as an inspiration for more complex SWG applications.

Index Terms ─ Broken-line SWG, energy leakage, metamaterials, Straight SWG, Surface-Wave Waveguide (SWG), tunable impedance cell.

I. INTRODUCTION

A surface wave is a type of electromagnetic wave that exists on the interface between metal and free space [1]. While propagating along the interface, they are restrained on the surface with their electric fields decaying exponentially along normal direction of the interface. According to the polarization of their electromagnetic fields, surface waves can be classified as transverse-magnetic (TM) or transverse-electric (TE), respectively.

Smooth metal surfaces support surface waves over a broad range of frequencies, spanning from DC up to visible light [1]. By applying a periodic texture, one can eliminate some surface waves over a finite frequency band. By purposely designing metal-dielectric periodic textures, one can change the effective impedance of the surface structure, and thus control the properties of the surface waves [2]. These surface structures with periodic textures are usually called impedance surfaces, and the unit-cell of the impedance surface is called an impedance cell, all of them are also called metamaterials.

Surface-wave waveguide (SWG) is a two-dimensional (2D) structure that guides the surface wave (SW) to propagate along a confined path [3]. Many articles have reported various SWGs. For instance, SWGs were designed based on pure metallic structures [4-5], plasmon structures [6], negative refraction or anisotropic chiral metamaterials [8-10], and impedance surfaces [3, 11-14]. The SWG based on impedance surfaces has become more and more popular because of its portability, economy and ease of processing.

The SWG can be used for various applications. For example, it can be utilized to transmit microwave energy [4-6], feed leaky-wave holographic antennas [7], and guide SW along a preferred path where they will not produce unwanted effects, such as scattering off objects into the surrounding space [3].

The remainder of this paper is organized as follows. The present research status of the SWG based on

Submitted On: January 20, 2016
Accepted On: March 10, 2016

impedance cells is given in Section II. Section III first briefly describes the unit-cell with tunable impedance properties, because it is the basis of the SWG that we proposed and several key data points must be obtained from it, and then it discusses in detailed theoretical models and analyzes ways of evaluating and suppressing energy leakage for the straight and broken-line SWG models. Numerical simulations and a discussion of the results have been done to verify our theory in Section IV. Finally, conclusions are drawn in Section V.

II. THE STATE OF ART

Gregoire and Kabakian reported that many SWGs, based on various-textured impedance cells in 2011, used textures that included a square with a slice through it, a rectangle, a diamond, and an anisotropic Jerusalem cross. Guided paths formed by these cells vary, such as straight, curved, and even hooked-shaped guide paths [3]. Quarfoth and Sievenpiper introduced the ray optics method to analyze the straight SWG model in 2011 [11], reported the simulation method of SWGs based on tensor impedance cells in 2013 [12], and then demonstrated two practical SWGs based on tensor impedance cells with a straight and arched guided paths, respectively, in 2015. Besides all these, Quarfoth analyzed the losses for a smooth bent SWG merely by the ray-optics method, in which the analysis process included a set of complicated equations [13].

All of above the mentioned research works are excellent, but the need still exist for their contents to be improved. For example, at least one common guided path has not be mentioned—the broken-line path. The broken-line SWG consists of several straight SWGs with heads-tails connecting in different directions on the same plane and it can replace the curved SWG. It is potentially advantageous over the curved SWG because its design and analysis are less complicated. Moreover, for SWGs, controlling energy leakage is very important since it determines the efficiency of surface wave propagation; however, as far as the authors' knowledge, no research on the analysis of the energy leakage has been reported. How to evaluate and suppress the energy leakage is not discussed either. Although the proposed ray-optics method has proved to be valid for the SWG made of impedance surface in some literatures. For instance, Quarfoth analyzed the losses for a smooth bent SWG by the ray-optics method in [13]. However, if we merely use this method to analyze the energy leakage of the straight and broken-line SWGs, the process will be very complicated.

In this work, by making use of the parallel plate waveguide theory together with the ray-optics method, several simple and effective equations will be acquired to forecast and control the energy leakage for the straight and broken-line SWGs. Moreover, by using surface-impedance-tunable cells introduced in our previous work [2], reconfigurable SWGs can be built with advantages such as low cost and multi-functionality. Furthermore, to judge whether the energy is leaky, a criterion of the energy leakage for the SWG is defined in this paper. Because the finite element method (FEM) had been verified in different domains [15-19], so all of numerical experiments of this paper are done in HFSS, a very popular commercial software based on the FEM.

III. METHODOLOGY

A. A brief introduction to the tunable impedance cell

The SWG can be regarded as a higher-impedance channel surrounded by two lower-impedance areas on a plane [12]. By utilizing tunable impedance cells properly, the SWG that we have proposed could now be built. From [22-25], the impedance of cells can be tuned by electric tuning or mechanical tuning. The goal of these two tuning methods is to change the equivalent capacitance of the cell. A modified slotted mushroom-like cell loaded with varactor diodes had been designed by us previously in [2], as shown in Fig. 1. On the top are a square metal patch, a square-ring-shaped metal patch and 4 varactor diodes across the slot. Five vertical vias are located on the patches, through the substrate, and isolated from the metal ground layer with clearances. Optimized dimensions of the structure are shown.

Spurred by TM surface waves, the measurement data indicated that its effective impedance ranges from j370 Ω to j780 Ω at 1.65 GHz when the bias voltage of varactor diodes decreases from 14 V to 2.3 V [2]. Using a simple voltage-switch, one can choose the impedance values of j370 Ω or j780 Ω. The circuit is also shown in Fig. 1.The impedance data and frequency of the unit-cell was adopted to perform the simulations in this paper.

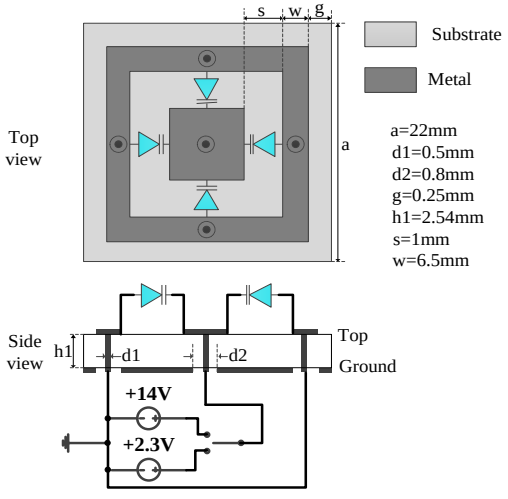

Fig. 1. The modified slotted mushroom-like unit-cell, not to scale. The central via is connected to a voltage of +2.3V or +14V for high or low impedance, respectively.

B. The topological structure of the SWG

An SWG based on impedance surface consisting of 30×30 tunable impedance units is modeled by HFSS, to illustrate multi-functionality, three different guiding paths on the same surface are exhibited in the figure, as shown in Fig. 2.

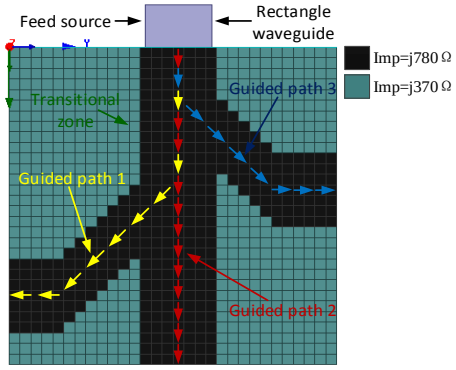

Fig. 2. Three different guided paths on the same impedance surface.

Obviously, from this figure we should notice that the curved path (path 1 or path 3) is just like a broken-line. Since the purpose of the SWG is to propagate surface waves with as little leakage as possible, it is reasonable to define a criterion for it. As for an antenna, S11 of its input port should be less than -10 dB. We believe the criterion of the energy leakage here should be stricter than return loss of antenna. Reference to return loss of antenna, if the ratio of the maximum electric field from outside to the inside of the SWG is converted to dB, the value (R) should be greater than -20 dB, or, $R = 20\lg(|E|_{\max\_outside} / |E|_{\max\_inside}) > -20dB$. It shows that the electromagnetic energy leaked from the black region to the blue region in Fig. 2 is larger than 1/100. In this case, the SW energy is considered to be leaky.

C. Theoretical models and analysis

A typical guided path (path 1 in Fig. 2) is chosen for theoretical analysis. To simplify the analysis, the stair-stepping boundary of the bent zone of the SWG is set to a straight line. The model in detail is shown in Fig. 3.

The whole guided path is a broken-line, but the front part is a straight line. According to the ray optics method, the propagation way of the TM surface wave in straight SWG is similar to that of the TM plane wave in parallel plate waveguide; both of them propagate by bouncing ways [11-13, 21]. Furthermore, it is clear that the parallel lines in Fig. 3 (for instance, y = 0 and y = d) are just like the profile of the parallel plate waveguide, therefore, the parallel plate waveguide theory is adopted to explain transmission properties of the TM surface-wave in straight SWG.

The width of the SWG is assumed to be d; the impedance of the inner zone is Z_1; the impedance of the outer zone is Z_2; and the angle between the wave vector of TM surface-waves (k) and z axial is θ. According to parallel plate waveguide theory [21],

$$k\sin\theta = \pi / d, \tag{2}$$

$$k = \omega\sqrt{\varepsilon\mu}, \tag{3}$$

where ω is the angular frequency of surface-wave, ε and μ are the effective dielectric constant and the effective magnetic conductivity of media, respectively. The light speed in media C_{media} is:

$$C_{media} = 1/\sqrt{\varepsilon\mu}. \tag{4}$$

From [2], the relation of surface impedance Z and the effective index of media n can be found,

$$Z = Z_0\sqrt{1-n^2}, \tag{5}$$

where Z_0 is the impedance of free space. Besides,

$$C_{media} = C_0 / n, \tag{6}$$

where C_0 is the light speed in free space.

By combining Equations (2) to (6), considering that $Z=Z_1$, we can figure out:

$$\theta = \sin^{-1}\left(\frac{\pi C_0}{d\cdot\omega\sqrt{1-\frac{Z_1^2}{Z_0^2}}}\right). \tag{7}$$

From Equation (7), different incident angles ϕ (complementary angle of θ) corresponding to different widths can be calculated as followed:

$$\phi = 90^\circ - \theta. \tag{8}$$

Based on the ray optics method [11-13], the critical angle $\alpha_{critical}$ can be solved when total inner refraction occurs.

$$\alpha_{critical} = \sin^{-1}\left(\frac{n_2}{n_1}\right) = \sin^{-1}\left(\frac{\sqrt{1-\frac{Z_2^2}{Z_0^2}}}{\sqrt{1-\frac{Z_1^2}{Z_0^2}}}\right). \tag{9}$$

According to the ray optics method, if $\phi \geq \alpha_{critical}$, then the leaky waves (energy leakage) in the straight zone would not appear.

When the waves arrive in the bent zone, leaky waves, if any occur, only appear on the outer-side boundary [13]. Just as Fig. 3 shows, we assume the bent angle is γ. According to geometry, we have:

$$\alpha + \theta + \gamma = 90^\circ. \tag{10}$$

Similarly, if $\alpha \geq \alpha_{critical}$, leaky waves in the bent zone would not appear either.

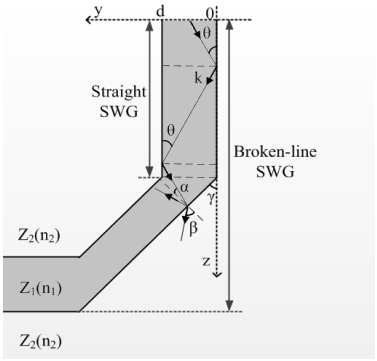

Fig. 3. Analyzing model of the SWG.

IV. RESULT ANALYSIS AND DISCUSSION

A. Computational results and analysis

According to Section II, let $Z_1 = j780\ \Omega$, $Z_2 = j370\ \Omega$ and $Z_0 = 377\ \Omega$ in Equation (9), $\alpha_{critical} = 37.6^\circ$ can be obtained. Incident angles corresponding to widths from 1×22 mm to 10×22 mm are calculated for straight and broken-line SWGs by the above equations, and the calculation results and the predictions of energy leakage are shown in Table 1 and Table 2, respectively.

Table 1: Incident angles corresponding to different width for the straight SWG

d (mm)	θ (degree)	ϕ (degree)	$\alpha_{critical}$ (degree)	Leak or Not
1×22	90-68.3j°	68.3j°	37.6°	Meaningless
2×22	64.1°	25.9°		Leaky
3×22	36.8°	53.2°		Not
4×22	26.7°	63.3°		Not
5×22	21.1°	68.9°		Not
6×22	17.4°	72.6°		Not
7×22	14.9°	75.1°		Not
8×22	13.0°	77.0°		Not
9×22	11.5°	78.5°		Not
10×22	10.4°	79.6°		Not

Table 2: Incident angles corresponding to different width for the broken-line SWG

d (mm)	θ (degree)	γ (degree)	α (degree)	$\alpha_{critical}$ (degree)	Leak or Not
1×22	90-68.3j°	45°	-45+68.3°	37.6°	Meaningless
2×22	64.1°		-19.1°		Leaky
3×22	36.8°		8.2°		Leaky
4×22	26.7°		18.3°		Leaky
5×22	21.1°		23.9°		Leaky
6×22	17.4°		27.6°		Leaky
7×22	14.9°		30.1°		Leaky
8×22	13.0°		32.0°		Leaky
9×22	11.5°		33.5°		Leaky
10×22	10.4°		34.6°		Leaky

From above tables, when the width of the straight SWG is less than 3×22 mm, the straight SWG begin to be leaky, however, the bent SWG is always leaky for all dimensions. Though θ is pure imaginary number in our calculation when d = 1×22 mm, we can't draw a conclusion directly from this result. Fortunately, because the leaky waves are obvious when d = 1×22 mm, we can infer that the leaky waves will appear heavily when d = 1×22 mm on the basis of Equation (6) and (7).

B. Simulation model and setup

In order to verify the theory, simulation experiments are performed. Based on [20], model of a straight SWG in HFSS is shown in Fig. 4. All the surfaces of the vacuum box are set to be radiation boundary except for the bottom surface. According to [2, 20], the rectangular waveguide WR-430 is used as feed source. All boundary conditions and feed source are the same for both straight and bent SWGs.

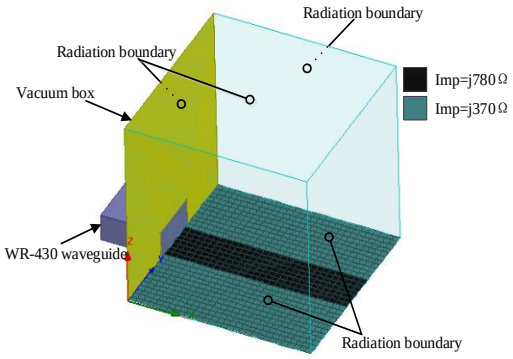

Fig. 4. Simulation model of a straight SWG in HFSS driven mode solver, not to scale.

C. Simulation results and analysis

For the straight SWG, path widths of 10×22, 6×22, 2×22, and 1×22 mm are chosen. The results have been demonstrated in Figs. 5 (a), (b), (c), and (d), respectively.

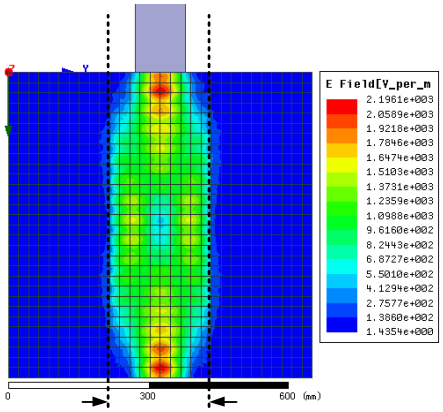

10×22(mm)

(a)

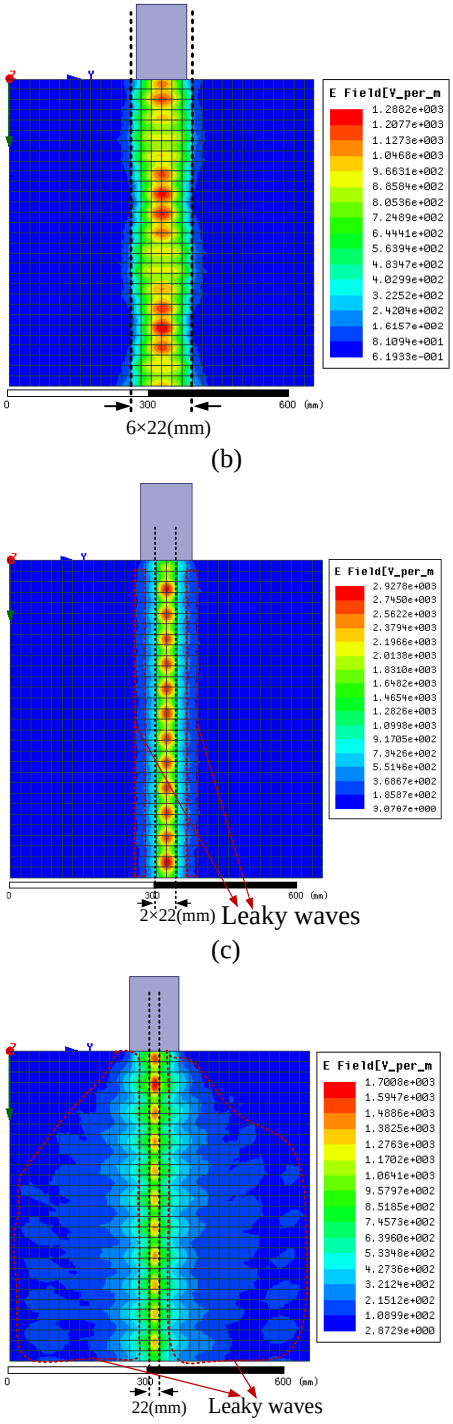

Fig. 5. Simulation results while d = 10×22 mm (a), 6×22 mm (b), 2×22 mm (c), and 1×22 mm (d).

From electric field data obtained by the simulation, we can calculate the ratio of the maximum electric field from outside o the inside of the SWG, respectively:

$$R_{10\times22} = 20\lg(150/2473) = -24.2dB < -20dB,$$

$$R_{6\times22} = 20\lg(93/1288) = -22.8dB < -20dB,$$

$$R_{2\times22} = 20\lg(368/2927) = -18dB > -20dB,$$

$$R_{1\times22} = 20\lg(533/1700) = -10dB > -20dB.$$

According to Equation (1), the latter two situations lead to energy leakage, which is completely in accordance with the theory. Moreover, it can be observed that the leakage increases as the width decreases.

For the broken-line SWG, according our theoretical forecast, the surface wave energy will always be leaky at the bent zone. The result is shown in Fig. 6.

According to Fig. 6, we can obtain that:

$$R_{6\times22\_b} = 20\lg(550/1863) = -10.6dB > -20dB.$$

The result demonstrates that the theory is correct.

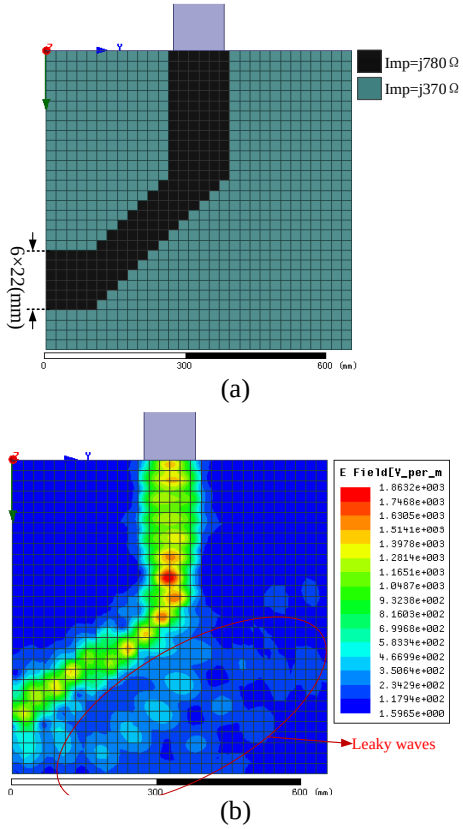

Fig. 6. Simulation model and result for the broken-line SWG with $Z_1 = j780\ \Omega$, (a) is model in HFSS, and (b) is simulation result.

What's more, the energy leakage can be suppressed further by increasing the impedance value of Z_1, while the other parameters remain the same. Specifically, in this case, the impedance range of Z_1 can be solved by combining Equations (6), (7), (8), and (9),

$$90^\circ - \gamma - \sin^{-1}\left(\frac{\pi \cdot C_0}{d \cdot \omega \sqrt{1+\frac{Z_1^2}{Z_0^2}}}\right) > \sin^{-1}\left(\frac{\sqrt{1-\frac{Z_2^2}{Z_0^2}}}{\sqrt{1-\frac{Z_1^2}{Z_0^2}}}\right). \quad (11)$$

Taking $\gamma = 45^\circ$, $d = 0.132$ m, $Z_0 = 377\ \Omega$, $Z_2 = 370\ \Omega$, and $f = 1.65$ GHz into Eq. 11. Through the numerical method, it can be obtained that Z_1 should be larger than $j970\ \Omega$. To guarantee a better suppression effect, we performed a simulation with $Z_1 = j1000\ \Omega$ in HFSS, and the simulation model and result are shown in Fig. 7.

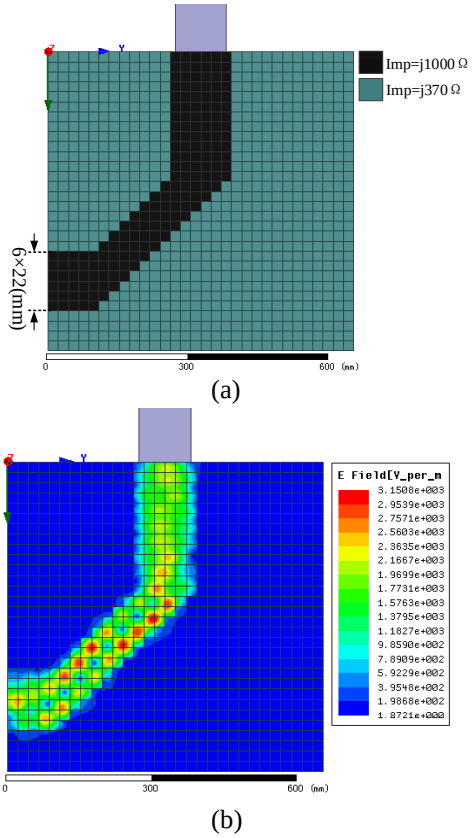

Fig. 7. Simulation result for the broken-line SWG with $Z_1 = j1000\ \Omega$; meanwhile the other parameters are unchanged, (a) is model in HFSS, and (b) is simulation result.

From Fig. 7, we can see that the leaky waves disappear. According to Equation (1), the ratio:

$$R = 20\lg(147/3150) = -26.6dB < -20dB,$$

which serves as a good example for the absence of leakage. Besides, we can draw another conclusion that the leakage decreases as the impedance of the guided path increases, and the leakage can be completely suppressed by increasing effective impedance of the guided path while the other parameters remain the same.

V. CONCLUSION

SWGs have been proposed for years, but their guiding efficiency, which is affected largely by surface wave leakage, has not been discussed thoroughly. To evaluate and suppress energy leakage for both straight and broken-line SWGs, simple and effective equations are derived. Differing from Quarfoth's analysis of the losses for a bent SWG, the analysis of the energy leakage for the proposed SWG is based on parallel plate waveguide theory and ray optics method in this paper, and the theory has been demonstrated to be evidently simpler and more effective. The multi-functionality of the SWG consisting of tunable impedance cells has been illustrated at the same time.

Structural parameters of the proposed SWG, such as the path width, incident angle, and effective impedance of guided path are analyzed in detail. The results are further verified by simulations, showing the satisfied accuracy of the theory. Besides that, a useful conclusion was arrived at, in that the leakage is inversely proportional to the width of the SWG and an increase of the effective impedance of the guided path. Furthermore, if the adjustment of other parameters for the proposed SWG is not convenient, one can control the energy leakage by increasing the impedance of the guided path. Although the results of HFSS are already very believable, measurement data always have more persuasive power, so our next work will be fabrication and testing to verify the contents of this paper.

ACKNOWLEDGMENT

The authors are thankful for financial support provided in part by the Youth Fund of the Education Department of Sichuan Province [Grant Number 11ZB031] and in part by a grant from China West Normal University [Grant Number CXTD2014-12].

REFERENCES

[1] D. F. Sievenpiper, "High-impedance electromagnetic surfaces," *Ph.D. Dissertation*, Dept. Electrical Engineering, Univ. California, Los Angeles, CA, USA, pp. 9-35, 1999.

[2] Z. Luo, X. Chen, J. Long, et al., "Nonlinear power-dependent impedance surface," *IEEE Transactions on Antennas and Propagation*, vol. 63, no. 4, pp. 736-1745, Apr. 2015.

[3] D. J. Gregoire and A. V. Kabakian, "Surface-wave waveguides," *IEEE Antennas and Wireless Propagation Letters*, vol. 10, pp. 1512-1515, 2011.

[4] W. Rotman, "A study of single-surface corrugated guides," *Proceedings of the IRE*, vol. 39, no. 8, pp. 952-959, Aug. 1951.

[5] R. Hougardy and R. Hansen, "Scanning surface wave antennas-oblique surface waves over a corrugated conductor," *IRE Transactions on*

Antennas and Propagation, vol. 6, no. 4, pp. 370-376, Oct. 1958.

[6] D. H. Lee and M.-H. Lee, "Gapped surface plasmon polariton waveguides for plasmonic signal modulation applications," *Journal of Nanoscience and Nanotechnology*, vol. 15, no. 10, pp. 7679-7684, Oct. 2015.

[7] B. Fong, J. Colburn, J. Ottusch, J. Visher, and D. Sievenpiper, "Scalar and tensor holographic artificial impedance surfaces," *IEEE Transactions on Antennas and Propagation*, vol. 58, no. 10, pp. 3212-3221, Oct. 2010.

[8] A. I. Ass'ad and H. S. Ashour, "TE magnetostatic surface waves in symmetric dielectric negative permittivity material waveguide," *Advances In Condensed Matter Physics*, Article Number: 867638, 2009.

[9] J. F. Dong, "Surface wave modes in chiral negative refraction grounded slab waveguides," *Progress In Electromagnetics Research, PIER 95*, pp. 153-166, 2009.

[10] J. R. Canto, C. R. Paiva, and A. M Barbosa, "Dispersion and losses in surface waveguides containing double negative or chiral metamaterials," *Progress In Electromagnetics Research, PIER 116*, pp. 409-423, 2011.

[11] R. Quarfoth and D. F. Sievenpiper, "Artificial tensor impedance surface waveguides," *IEEE Transactions on Antennas and Propagation*, vol. 61, no. 7, pp. 3597-3606, Jul. 2013.

[12] R. Quarfoth and D. Sievenpiper, "Impedance surface waveguide theory and simulation," *Proceedings of the 2011 IEEE Antennas and Propagation Society International Symposium and USNC/URSI National Radio Science Meeting*, pp. 1159-1162, Jul. 2011.

[13] R. G. Quarfoth and D. F. Sievenpiper, "Nonscattering waveguides based on tensor impedance surface," *IEEE Transactions on Antennas and Propagation*, vol. 63, no. 4, pp. 1746-1755, Apr. 2015.

[14] R. Quarfoth and D. F. Sievenpiper, "Simulation of anisotropic artificial impedance surface with rectangular and diamond lattices," *Proceedings of the 2011 IEEE Antennas and Propagation Society International Symposium and USNC/URSI National Radio Science Meeting*, pp. 1498-1501, Jul. 2011.

[15] A. Saldana-Robles, E. Aguilera-Gomez, H. Plascencia-Mora, et al., "Three-dimensional modeling of surface roughness for burnishing process," *DYNA*, vol. 90, no. 4, pp. 423-432, Jul.-Aug. 2015.

[16] D. A. Mantaras and P. Luque, "Assessing motorcyclist protection systems using finite element simulations," *International Journal of Simulation Modelling*, vol. 14, no. 1, pp. 110-120, Mar. 2015.

[17] B. Cirkovic, I. Camagic, and N. Vasic, "Analysis of the supporting structure of composite material tool machine using the finite element method," *Tehnicki Vjesnik*, vol. 22, no. 1, pp. 95-98, Feb. 2015.

[18] S. Shabazpanahi, A. A. A. Ali, F. N. Aznieta, et al., "Finite element modeling of crack propagation in RC beam by using energy approach," *Journal of Engineering Science and Technology Review*, vol. 7, no. 1, pp. 65-70, 2014.

[19] K. Lubikowski, S. Radkowski, K. Szczurowski, et al., "Seebeck phenomenon, calculation method comparison," *Journal of Power Technologies*, vol. 95, no. 2015, pp. 63-67, 2015.

[20] Z. Luo, X. Chen, J. Long, et al., "Self-focusing of electromagnetic surface waves on a nonlinear impedance surface," *Applied Physics Letters*, vol. 106, no. 21, pp. 2111021-5, May 2015.

[21] D. M. Pozar, *Microwave Engineering*, Third Edition, John Wiley & Sons, pp. 85-88, 2005.

[22] D. Sievenpiper and J. Schaffner, "Beam steering microwave reflector based on electrically tunable impedance surface," *Electronics Letters*, vol. 38, no. 21, pp. 1237-1238, Oct. 2002.

[23] R. S. Schofield, J. C. Soric, D. Rainwater, et al., "Scattering suppression and wideband tunability of a flexible mantle cloak for finite-length conducting rods," *New Journal of Physics*, vol. 16, Article Number: 063063, Jun. 2014.

[24] D. Sievenpiper, J. Schaffner, J. J. Lee, et al., "A steerable leaky-wave antenna using a tunable impedance ground plane," *IEEE Antennas and Wireless Propagation Letters*, vol. 1, pp. 179-182, 2002.

[25] H. Liu, S. Gao, and T. H. Loh, "Low-cost beam-switching circularly-polarised antenna using tunable high impedance surface," *Proceedings of the 2012 Loughborough Antennas & Propagation Conference (LAPC)*, Nov. 2012.

Yonghong Zhou received his M.S. degree in Computer Applications Technology from Southwest Petroleum University, Chengdu, China, in 2005. He is currently pursuing Ph.D. in Radio Physics at Sichuan University. He joined the teaching staff in 2005 and is currently an Associate-Professor with the College of Electronics and Information Engineering, China West Normal University. His research area includes surface

wave metamaterials and numerical methods applied in electromagnetics.

Xing Chen received the M.S. degree in Radio Physics and the Ph.D. degree in Biomedical Engineering from Sichuan University, Sichuan, China, in 1999 and 2004, respectively. He joined the teaching staff in 1991 and is currently a Professor with the College of Electronics and Information Engineering, Sichuan University. His main research interests are in the fields of antenna, microwave imaging, global optimization, numerical methods applied in electromagnetics, and parallel computation. Chen is a Senior Member of the Chinese Institute of Electronics.

Zhangjie Luo received his B.S. degree in Electronic and Information Engineering and the Ph.D. degree in Radio Physics from Sichuan University, Chengdu, China, in 2008 and 2015, respectively. He is currently a Research Staff with the Institute of Electronic Engineering, China Academy of Engineering Physics. From 2012 to 2014, he worked in the Applied Electromagnetics Group at the University of California, San Diego, USA, as a visiting Ph.D. student. His research area includes surface wave metamaterials, circular waveguides, and microstrip antennas.